Fine-scale environment control on ground surface temperature and thaw depth in a High Arctic tundra landscape

Hadi Mohammadzadeh Khani, Christophe Kinnard, Simon Gascoin, Esther Lévesque

Received: 26 October 2021 | Revised: 6 June 2023 | Accepted: 1 July 2023

DOI: 10.1002/ppp.2203

RESEARCH ARTICLE

WILEY

Fine-scale environment control on ground surface temperature and thaw depth in a High Arctic tundra landscape

Hadi Mohammadzadeh Khani[1,2] | Christophe Kinnard[1,2] | Simon Gascoin[3] | Esther Lévesque[1,2]

[1]Centre de Recherche sur les Interactions Bassins Versants—Écosystèmes Aquatiques (RIVE), Département des Sciences de l'Environnement, Université du Québec à Trois-Rivières, Trois-Rivières, Quebec, Canada

[2]Centre d'Études Nordiques (CEN), Quebec, Quebec, Canada

[3]Centre d'Études Spatiales de la Biosphère (CESBIO), Université de Toulouse, CNRS/CNES/IRD/INRAE/UPS, Toulouse, France

Correspondence
Hadi Mohammadzadeh Khani, Centre d'Études Nordiques (CEN), Quebec, Quebec, Canada.
Email: hadi.mohammadzadeh.khani@uqtr.ca

Funding information
Natural Sciences and Engineering Research Council of Canada, Grant/Award Numbers: RGPIN-2015-05319, RGPIN-2015-03844; Canada Research Chair program, Grant/Award Number: 231380; Centre de Recherche sur les Interactions Bassins Versants—Écosystèmes Aquatiques (RIVE)

Abstract

Surface conditions are known to mediate the impacts of climate warming on permafrost. This calls for a better understanding of the environmental conditions that control the thermal regime and the depth of the active layer, especially within heterogeneous tundra landscapes. This study analyzed the spatial relationships between thaw depths, ground surface temperature (GST), and environmental conditions in a High Arctic tundra environment at Bylot Island, Nunavut, Canada. Measurements were distributed within the two dominant landforms, namely earth hummocks and low-center polygons, and across a topographic gradient. Our results revealed that GST and thaw depth were highly heterogeneous, varying by up to 3.7°C and by more than 20 cm over short distances (<1 m) within periglacial landforms. This microscale variability sometimes surpassed the variability at the hillslope scale, especially in summer. Late-winter snowpack thickness was found to be the prime control on the spatial variability in winter soil temperatures due to the highly heterogeneous snow cover induced by blowing snow, and this thermal effect carried over into summer. However, microtopography was the predominant driver of the spatial variability in summer GST, followed by altitude and moss thickness. In contrast, the spatial variability in thaw depth was influenced predominantly by variations in moss thickness. Hence, summer microclimate conditions dominated active layer development, but a thicker snowpack favored soil cooling in the following summer, due to the later disappearance of snow cover. These results enhance our understanding of High Arctic tundra environments and highlight the complexity of considering surface feedback effects in future projections of permafrost states within heterogeneous tundra landscapes.

KEYWORDS
ground surface temperature, High Arctic, landscape heterogeneity, permafrost active layer, snow cover, thaw depth

1 | INTRODUCTION

The High Arctic (HA) has experienced unprecedented changes over the last three decades.[1–3] Recent studies and observations have shown that permafrost (soil or rock at or below 0°C for at least two consecutive years[4]) is warming and thinning over Arctic regions, including the HA.[5–8] Over the past 50 years, climate change has led to a reduction in permafrost extent, increasing permafrost temperature, and an increase in

active layer thickness (ALT), "the top layer of soil that thaws in summer and refreezes in winter".[9] Permafrost thawing leads to a deeper active layer, which modifies the surface and subsurface hydrology, and impacts aquatic and terrestrial ecosystems and northern traditional lifestyles.[10] Permafrost thawing also modifies the configuration of existing lakes, streams, and rivers, and creates new freshwater ecosystems.[11] Active layer deepening can also amplify climate change at a global scale, due to the release of stored soil organic carbon to the atmosphere.[8]

Although climatic warming is important in driving permafrost thawing and in increasing ALT, surface (vegetation and snow) and subsurface (soil) conditions are the main local drivers of the seasonal response of permafrost to climate.[2,12,13] To accurately project the effects of climate change on permafrost and related ecosystem functions, a good understanding of surface feedback processes and their spatial scales of occurrence is needed, so that these processes may be better represented within models.[14,15]

The development of a seasonal active layer is a temporally dynamic and spatially heterogeneous process, due to the spatial variations in topography, vegetation, and soil conditions.[16,17] Vegetation in the HA is often dominated by a heterogeneous covers of moss and lichen, which form an insulating layer overlying the mineral soil.[18] During summer, the ground surface is buffered from air temperatures by the vegetation cover that shades and cools the underlying soil. Vegetation also increases the surface roughness, which increases evapotranspiration and further cools the soil.[19–21]

While summer climate and surface conditions are key drivers of active layer development, winter preconditioning effects can also be important. Snow cover insulates the ground from low winter temperatures, which delays cooling of the underlying soil in winter, while in the spring a longer lasting snow cover delays ground warming and thawing.[22–24] In HA tundra landscapes devoid of erect vegetation, the snow cover is thin and continuously redistributed by the wind into topographic depressions, resulting in pronounced snow cover heterogeneity. As such, the micro-relief often represents a substantial fraction of the variability in total snow depth.[19] Microtopography has also been shown to impact the structure and thermal characteristics of the snow and underlying ground.[25]

While the impact of surface and subsurface conditions (snow, vegetation, and soil) on thaw depths and ground surface temperatures (GSTs) have been well studied at the hillslope scale (e.g.,[26–28]), microscale variability has been comparatively less well studied, although it can control the response of permafrost to climate change at larger scales.[25,29–31] There is thus a need to better characterize and understand the spatial interactions between active layer thermal states and their environmental drivers to better constrain land surface feedbacks on climate-driven permafrost thawing and carbon release.[32] While process-based models are useful to disentangle climate and land cover impacts on ALT and temperatures, statistical modeling represents a useful and alternative step for this purpose.[4] The objective of this study was thus to assess the influence of environmental conditions (topography, snow, vegetation, and soil) on the spatial variability of GST and thaw depth at two spatial scales (microtopographic and hillslope scales) in an HA tundra landscape.

2 | DATA AND METHODS

2.1 | Study site

The study area is located in an HA tundra environment on the western plain of Bylot Island, off the northern coast of Baffin Island in Nunavut, Canada (Figure 1). The study site is situated on the hillslope ranging in elevation from 20 to 350 m a.s.l. and underlain by an ~400-m-thick continuous permafrost.[33] The land surface consists of mineral-earth hummocks and low-center polygons (Figure 1). The prostrate vegetation is relatively diverse for this latitude, with more than 166 vascular plant species and a rich bryophyte flora.[34] Wetlands occur generally at lower elevations with both high- and low-centered polygons dominated by sedges (*Carex aquatilis*, *Eriophorum angustifolium*, *Eriophorum scheuchzeri*), grasses (*Dupontia fisheri*, *Pleuropogon sabinei*), and fen mosses (*Drepanocladus* spp.).[35–37] Mesic environments, found across a broad range of conditions including low-centered polygon rims, gently sloping terrain, and hummocky tundra, support a more diverse group of species including *Salix* spp., *Vaccinium uliginosum*, *Arctagrostis latifolia*, *Poa arctica*, and *Luzula confusa* with *Aulacomnium* spp. as the dominant moss species.[38] Annual mean temperature at the Bylocamp station (Table S1), operated by the Center for Northern Studies (CEN), was −15.1°C for the period 1981–2010, with a noticeable warming trend over the last five decades.[39] Annual precipitation over the same period was 191 mm, mostly (76%) falling as snow. The annual average winter snowpack typically reaches 35–45 cm and snow accumulation is spatially variable due to topographic heterogeneity and winter snow drifting from predominant easterly winds.[40,41]

2.2 | Air temperature, GST, and thaw depth measurements

The air temperature was measured at the Bylocamp station during 2016–2018 at 1-h intervals, and the data were retrieved from the Nordicana website.[39] GST was measured continuously from July 1, 2016 to July 1, 2018 (730 days) at a network of 100 temperature micro data loggers (Figure 1). Loggers were small (<2 cm) iButtons (DS1922L model) with a 0.5°C accuracy and set at a 3-h sampling interval. The loggers were installed at 3 cm below the ground surface (bare soil or moss) to avoid direct insolation during the snow-free season. The moss cover was considered part of the ground rather than part of the vegetation canopy so some of the loggers were recording the temperature inside mosses. The objective of the sampling design was to efficiently distribute the available loggers across the range of elevation and slope aspects and over contrasting morphological features (hummocks, polygons) (Figure 1). Eighteen hummocks and seven low-centered ice-wedge polygons were chosen randomly. More loggers were allocated to hummocks as these landforms are predominant at the site. Loggers were deployed at the top and bottom of the hummocks (18 pairs) and on the rims and centers of the polygons (seven pairs). The remaining loggers were distributed over mostly flat terrain

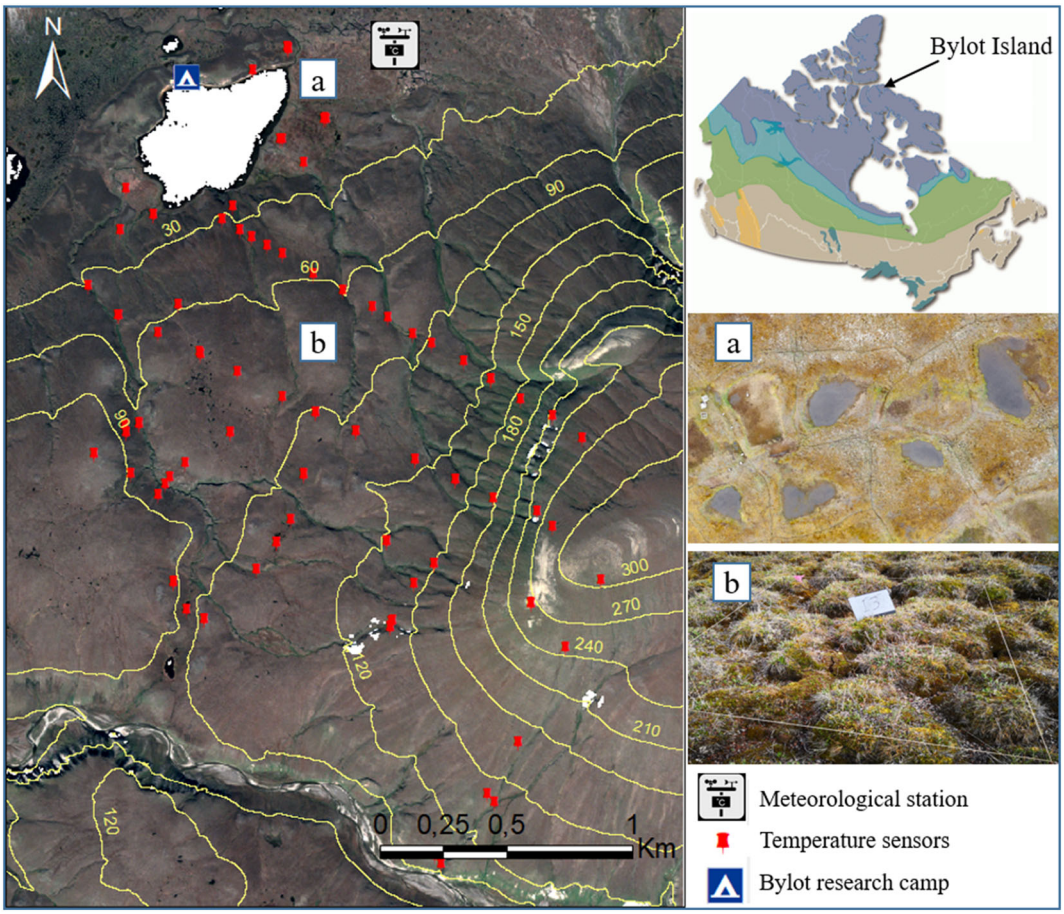

FIGURE 1 Study area and site. Top right: general location of Bylot Island on the Canada permafrost map[7]; left: map of study area showing the location of automatic weather stations and the sites with ground surface temperature sensors. Image source: Pléiades © CNES 2016 Distribution Airbus DS. (a) Drone aerial photo of low-center polygons and (b) photo of earth hummocks. [Colour figure can be viewed at wileyonlinelibrary.com]

(Table S2). The position of each logger was recorded with a differential global navigation satellite system (FOIF A30 GNSS) with ±1-cm accuracy. The loggers were collected in early July 2018, and GST data were retrieved. The second year of data was excluded from the analysis because the loggers were removed in early July 2018, shortening the representation of summer GSTs. Of the 100 loggers deployed, seven were lost or broken, leaving 93 available for analysis. Thaw depth (ThawD) was measured twice per season at each logger, in early July and late August, using a graduated steel rod with a ±0.5-cm precision on readings. Thaw depths obtained by probing could be affected by the presence of rocks; however, extensive soil sampling in the summer of 2018 revealed mostly fine-textured soils down to 1 m.

2.3 | Environmental variables, topoclimatic variables, and meteorological data

Environmental variables including vegetation type and cover, soil moisture, and texture were measured sporadically next to all temperature loggers during summers of 2016 and 2017, while snow depth was measured during late winter 2017 (Table 1). The portion of ground covered either by bare soil or by vegetation was estimated visually within a 2 × 2-m plot centered around each logger in summer 2017 using cover classes (0–1%, 1–5%, 5–10%, 10–25%, 25–50%, 50–75%, >75%). Vegetation cover was measured separately for deciduous shrubs, evergreen shrubs, graminoids, forbs, mosses, lichens, and cryptogamic crust. To simplify the statistical analyses, the measured vegetation types were merged into three groups: vascular plants (including deciduous shrubs, evergreen shrubs, graminoids, and forbs), mosses, and lichen–cryptogamic crust. The cover per strata was calculated as the sum of the mid class value.[42] Vegetation cover can exceed 100% because some vegetation strata overlap each other inside the plot. The thickness of organic material and moss cover (both dead and live) were measured at each logger location. Near-surface soil moisture (top 10 cm of the soil) was measured twice per season at each logger, in early July and late August, using a time-domain reflectometry (TDR) moisture probe (Delta-T HH2, 4% accuracy on volumetric water content). A distinct TDR probe calibration was used for organic and mineral soils, based on a preconfigured probe calibration. Soil texture classes were identified onsite using the manual ("feel") method.[43,44] A 2-m-resolution digital elevation model (DEM) built from Pleiades stereo images acquired on July 28, 2016 was used to calculate topographic indices across the study site including slope and aspect. The DEM was generated using the Ames Stereo Pipeline[45]

TABLE 1 Environmental variables measured at the logger (*j*) and site (*i*) levels.

Variable	Definition	Unit	Range	Measurement method
Alt_j	Altitude	m	20–325	GNSS
Slp_i	Slope	°	0–90	DEM
WE_i	Eastern exposure	—	−1 to +1	sin (aspect)
SN_i	Northern exposure	—	−1 to +1	cos (aspect)
$MicT_j$	Microtopography index: (exposed = 1, sheltered = 0)	Binary	0 or 1	Field interpretation
Rad_i	Mean summer potential solar radiation	WH/m^2	—	ArcGIS
$VegT_j$	Dominant vegetation type	—	5 types	2 × 2-m plot
$VegC_i$	Vegetation cover (moss, vascular plants, lichen, and cryptogamic crust)	%	0 to 100	2 × 2-m plot
$MossT_j$	Moss thickness	cm	0 to 5	2 × 2-m plot
$SoilMJ_j$	Soil moisture at the beginning of July	%	0 to 100	TDR sensor
$SoilMA_j$	Soil moisture at the end of August	%	0 to 100	TDR sensor
$SoilT_j$	Soil texture	—	6 types	"Feel" method
$ThawD_j$	Thaw depth at the end of August	cm	20 to 150	Steel probe
SD_j	End-of-winter snow depth	cm	20 to 180	Steel probe
SDD_j	Snow disappearance date	Day of year	240 to 255	From GST records
SOD_j	Snow onset date	Day of year	165 to 190	From GST records
Ta	Air temperature	°C	−45 to 22	YSI 44033 sensors (1-h interval)
$T_{win,\,j}$	Winter ground surface temperature at 3-cm depth	°C	−40 to 0	iButtons sensors (3-h interval)
$T_{sum,\,j}$	Summer ground surface temperature at 3-cm depth	°C	0 to 15	iButtons sensors (3-h interval)

using the same configuration as in a previous study in the Pyrenees mountains.[46] Snow depth was measured continuously at the Bylocamp station (Figure 1) by using an ultrasonic gauge (Campbell Scientific SR50 with an accuracy of ±1 cm) while GST was measured at 2 cm below the surface via a Campbell Scientific 107 probe. Snow depth was measured by probing at each logger in 2017 close to the approximate time of maximum snow accumulation based on recorded snow depth at the Bylocamp station (May 1–7, 2017). In addition to end-of-winter snow depth measurements, the snow disappearance date (SDD) and snow onset date (SOD) were estimated at each micro-logger based on the 3-hourly GST records, following the methods from Staub and Delaloye.[47] A full description of the extraction of snow cover duration indices and their calibration and validation is given in Appendix S1. SOD and SDD were further used to define the summer and winter periods in the statistical analyses. The mean SDD of all the loggers was determined to be the start of the summer season in order to discretize the seasonal ground temperature between summer and winter.

2.4 | Statistical analyses

2.4.1 | Microtopographic-scale (logger-level) analysis

A nonparametric Wilcoxon signed-rank test was applied to test whether significant differences in GST and thaw depth occurred between exposed locations (hummock tops and polygon rims) and more sheltered locations (hummock troughs and polygon centers). In addition, a Fisher variance ratio test (*F* test) was used to compare the within-landform (logger-level) versus among landform (site-level) spatial variability in GST and thaw depth.

2.4.2 | Hillslope-scale (site-level) analysis

Redundancy analysis (RDA) was used to explore the potential relationships between response variables (summer GST: T_{sum}, winter GST: T_{win}, and thaw depth: ThawD) and explanatory environmental variables. RDA finds the multidimensional axes that explain most of the variation in the response variables and that are explained by the independent, spatial environmental variables.[48] For sites with paired loggers, GST records from both loggers were averaged in this analysis. Site and variable scores were displayed on triplots using "type-II scaling," emphasizing the correlative relationships between variables.[49] The significance of the overall RDA model and individual RDA axes was assessed with a permutation test.[50] Prior to RDA, all numerical variables were transformed to a normal distribution using square root and log transformations and then centered to their means.[48] Because our data include binary variables, the continuous variables were scaled by twice the standard deviations so that the range of continuous variables is more similar to the range of binary variables.[51]

2.4.3 | Multilevel analysis

The spatial variables which affect GST and thaw depth were explored using multilevel regression models, or "mixed models."[52] Multilevel models account for grouping in observations; these grouping variables are known as random effects and can account for correlation in residuals within the groups.[53] In this study, each logger represents an observation, which can be grouped within a site, that is, where pairs of loggers were installed within periglacial landforms. Random-intercept multilevel models were thus developed to predict GST and thaw depth from spatial environmental variables (fixed effects) with site as the grouping variable (or "random effect") using the lme4 package in R.[54] The same data transformations and standardization used for RDA were applied on the predictor variables in order to compare their relative contribution within the models. Multicollinearity was assessed with the variance inflation factor (VIF) and pairwise correlations among predictors.[55] Predictors with a VIF >10 or a pairwise correlation >0.7 were flagged as collinear and discarded from the multilevel analysis. A model was developed for each dependent variable, that is, T_{sum}, T_{win}, and maximum thaw depth, as measured in late August. A full model was first constructed using all fixed and random effects. This global or "beyond optimal" model was then simplified by sequentially removing nonsignificant predictors ($p < 0.05$).[52] Conditional and marginal pseudo coefficients of determination (R^2) were used to evaluate model fit. The marginal pseudo-R^2 reflects the proportion of variance explained by the fixed environmental effects only, while the conditional pseudo-R^2 also includes the random (site) effect.[56] Model residuals were analyzed to check model assumptions for normality, homogeneity of variance, and independence. Table 1 lists all the variables used within the RDA and multilevel analyses.

3 | RESULTS

3.1 | Variations of GST, thaw depth, and environmental variables

Mean daily air temperature at the Bylocamp station varied between −45 and 1°C in winter and between −1 and 18°C during summer for the hydrological year 2016–2017. Mean daily ground temperature varied across the logger sites from −18.3 to −6.1°C during winter and from 2.7 to 11.8°C during summer (Figures 2 and S3). The thaw depth probed in August varied from 20.5 to 80 cm across sites.

The snowpack typically started to accumulate in early September and melted out by mid-June (Figure 2). Snow accumulation reached a maximum of 70 cm on May 10, 2017, at the Bylocamp weather station, while end-of-winter snow depths varied between 17 and 156 cm across the logger sites. This strong spatial variability in snow depth reflects the influence of blowing snow redistribution. The snowmelt period was short, typically lasting 2 weeks (Figure 2). The spatial

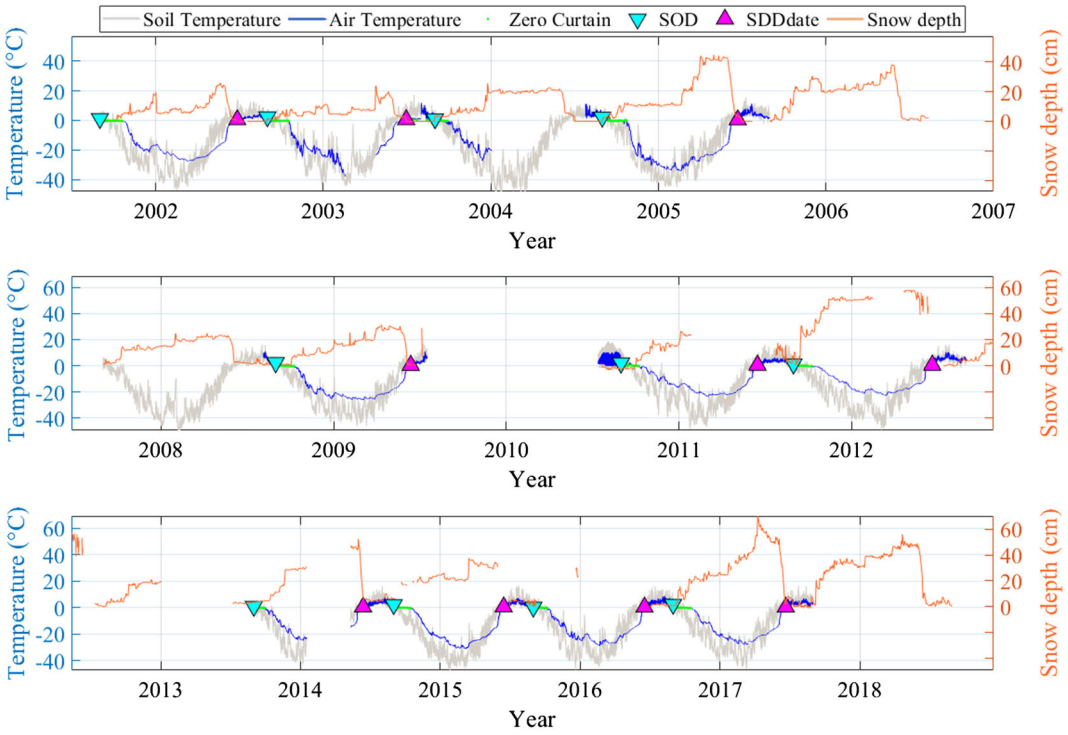

FIGURE 2 Air and ground temperature records at the Bylocamp station. The snow onset dates (SOD) and snow disappearance dates (SDD) were calibrated on the ground temperature records during the period 2002–2008 and validated during 2009–2018. The brown line represents daily snow height, the blue line represents ground surface temperatures, and the gray line represents daily air temperature with a 3-h interval. The estimated SOD and SDD are indicated as cyan and purple triangles, respectively, while green dots indicate zero-curtain (ZC) periods. [Colour figure can be viewed at wileyonlinelibrary.com]

variability of SOD across sites (standard deviation = 13 days) was larger than that of SDD (9 days). The total vegetation cover around the loggers varied from 34 to 145% with 3–88% for mosses and 3–63% for vascular plants (Figure S1). Moss thickness varied from 1.8 to 4.5 cm.

3.2 | Microscale variability in GST

No significant difference in annual GST was found between exposed and sheltered locations for hummocks (median difference between tops and bottoms = 0.22°C, $p = 0.38$) and polygons (median difference between rims and centers = 0.74°C, $p = 0.06$) (Table 3). However, significant seasonal differences were found for hummocks, with the exposed tops being colder than the sheltered bottoms in winter (median difference = 0.60°C, $p = 0.01$), and warmer than the bottoms in summer (median difference = 1.95°C, $p < 0.001$) leading to significantly deeper thaw depths on hummock tops compared to bottoms (by 13.2 cm, $p < 0.001$) while no difference was found in GST within polygons at the seasonal scale, yet thaw depth was significantly deeper in the centers compared to the rims (by 13.7 cm, $p = 0.01$, Table 2).

The spatial variability in mean annual GST at hummocks sites was significantly greater among sites than within the hummocks ($F = 0.07$, $p < 0.001$), while there was no significant difference for polygons ($F = 0.68$, $p = 0.211$) (Table 2). In winter, GST for hummocks was more variable among sites than within the hummocks ($F = 0.45$, $p < 0.001$) but this pattern reversed in summer: GST varied slightly more at the microscale (within hummocks) than at the hillslope scale, where the difference between the warmer tops and colder bottoms can be ascribed to micro-topographic shading and differences in soil moisture. For polygons, GST varied more among sites in summer ($F = 0.36$, $p = 0.018$) but more within polygons in winter ($F = 2.05$, $p = 0.069$). The variability in thaw depth was similar at the microscale and hillslope scale for both polygons and hummocks (Table 2). These results show that at the seasonal scale, the microscale (within-site) variation can surpass variability at the hillslope scale.

3.3 | Hillslope-scale (site-level) heterogeneity analysis

Results from the RDA show that 61.1% of the variation in the response variables (T_{win}, T_{sum}, and ThawD) at the site level was constrained by the variation of the environmental variables in the first three axes (Table 3). However, permutation tests showed that only the first two RDA axes were significant ($p < 0.001$), respectively accounting for 37.1 and 16.9% of the variance of the dependent variables. The first two RDA axes clearly separate the site scores and explanatory variables according to processes associated with the winter (Axis 1) and the summer (Axis 2) seasons (Figure 3 and Tables 3 and S4). However, the variance of the two dominant axes (54%) means that site-level GST and thaw depth variability is not entirely explained by the existing environmental variables.

Axis 1 is characterized by positive relationships of T_{win} with snow depth (SD), SDD, and topographic slope (Slp), and to a lesser extent July and August soil moisture (SoilMJ and SoilMA) while also showing a weak inverse relationship with solar radiation (Rad) (Table 3 and Figure 3). The small but positive effect of altitude on T_{win} results in

TABLE 2 Annual and seasonal ground surface temperature (GST) and maximum thaw depth (ThawD) within and among dominant microscale landforms.

Wilcoxon test						
	Median: hummocks ($n = 18$)			**Median: polygons ($n = 7$)**		
Period	**Top**	**Bottom**	***p* value**	**Rim**	**Center**	***p* value**
Annual GST (°C)	−11.4	−11.2	0.38	−11.5	−10.7	0.06
Winter GST (°C)	−15.4	−14.8	0.01	−15.7	−14.6	0.69
Summer GST (°C)	5.2	3.3	<0.001	4.5	6	0.16
ThawD (cm)	37.6	24.4	<0.001	23.3	37.0	0.015
Fisher test						
	Standard deviation: hummocks ($n = 18$)			**Standard deviation: polygons ($n = 7$)**		
Period	**Within**	**Among**	***F***	***p***	**Within**	**Among**	***F***	***p***
Annual GST (°C)	0.27	1.04	0.07	<0.001	0.67	0.81	0.68	0.211
Winter GST (°C)	0.45	1.24	0.13	<0.001	0.96	0.67	2.05	0.069
Summer GST (°C)	1.02	0.83	1.51	0.2	0.73	1.22	0.36	0.018
ThawD (cm)	8.7	9.8	0.78	0.62	8.2	8.0	1.04	0.96

Note: Differences in GST and ThawD between exposed (hummock tops and polygon rims) and sheltered (hummocks bottoms and polygon centers) locations were assessed with the Wilcoxon sign rank test. The spatial variability of GST and ThawD was partitioned into within- and among-landform variability and the variance ratio (within/among) tested with the Fisher variance test (*F* test).

TABLE 3 Results from the redundancy analysis (RDA) of the inter-site spatial variability of thaw depth and summer and winter GST.

Partitioning of correlations						
		Variance			Proportion	
Total		3			1	
Constrained		1.836			0.6118	
Unconstrained		1.164			0.3882	
Eigenvalues and their contribution to the correlations						
	RDA1	RDA2	RDA3	PC1	PC2	PC3
Eigenvalues	0.278	0127	0.053	0.185	0.065	0.041
Proportion explained	0.371	0.169	0.071	0.246	0.087	0.055
Cumulative proportion	0.371	0.54	0.611	0.858	0.945	1
Accumulated constrained eigenvalues						
	RDA1		RDA2		RDA3	
Total	0.278		0127		0.053	
Constrained	0.606		0.277		0.116	
Cumulative proportion	0.606		0.883		1.00	
Response variable scores						
	RDA1	RDA2	RDA3	PC1	PC2	PC3
Thaw depth	1.297	−0.116	−0.402	0.126	0.346	0.547
T_{win}	−0.559	0.75	−0.438	1.01	0.41	−0.216
T_{sum}	−0.746	0.765	0.369	0.819	0.556	0.18

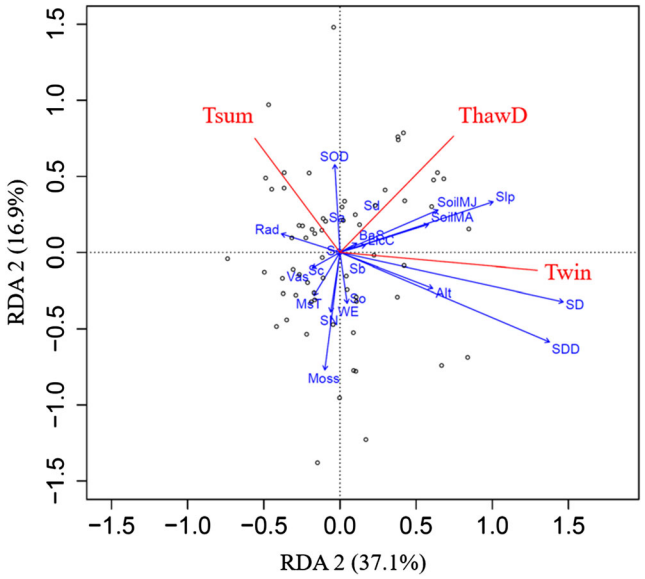

FIGURE 3 Triplot for RDA1 and RDA2 axes. Red arrows: dependent variables (winter ground temperature [T_{win}], summer ground temperature [T_{sum}], thaw depth [ThawD]); blue arrows: independent variables; dots: site scores. The angles between arrows reflect the linear correlation between variables. Soil types (S) are: Sa, gravely soil; Sb, sandy soil; Sc, sandy loam soil; Sd, loamy soil; Se, clay soil; So, peat soil. Snow cover indices are snow onset date (SOD), snow disappearance date (SDD), and snow depth (SD). Vegetation parameters are moss thickness (MsT), moss cover (Moss), vascular plants (Vas). Topographic parameters include solar radiation (Rad), northern exposure (SN), and eastern exposure (WE). [Colour figure can be viewed at wileyonlinelibrary.com]

the valley bottom being colder than upslope areas in winter, presumably due to cold air pooling and the resulting positive winter lapse rate (Figure S2). Hence, the spatial heterogeneity of T_{win} at the hillslope scale is controlled primarily by the spatial variability of the late-winter snow depth, and by solar radiation.

Axis 2 is mainly defined by negative relationships between summer GST (T_{sum}) and moss thickness (MossT), moss cover, and WE and SN aspect (Figure 3). Hence, a thicker and more extensive moss layer promoted cooler soils in summer. T_{sum} is also positively correlated, albeit weakly, with solar radiation, and negatively correlated with altitude and snow depth. Hence, lower air temperatures promoted cooler soils at higher elevation in summer, in accordance with the negative summer lapse rate (Figure S2). The negative correlation between T_{sum} and snow depth shows that sites with thicker snowpacks tended to be cooler in summer.

ThawD is loaded positively both on the "winter" (RDA1) and "summer" (RDA2) axes (Figure 3), suggesting that both winter processes and summer conditions influenced thaw depths at the hillslope scale. Thaw depth notably displays a positive correlation with early and late summer surface moisture, with greater thaw depth occurring at wetter sites (Figure 3). Sites with greater thaw depths were also associated with increased topographic slope, as well as thinner moss cover and lower vascular and moss vegetation cover (Figure 3). Solar radiation was poorly correlated with all three RDA axes, and no clear influence of soil type on GST or thaw depth was found (Table S4 and Figure 3).

3.4 | Multiscale environmental control on thaw depth and seasonal GST

The preliminary collinearity test identified three redundant potential predictors, namely SDD (collinear with SD), measured soil moisture in July (SoilMJ: collinear with measured soil moisture in August), and SN (collinear with solar radiation) (Figure S4). SN and SoilMJ were dropped, while SDD was dropped for the T_{win} model but kept for the T_{sum} model since it is more physically linked to summer GST than SD. The model selection procedure described in the methods section led to the following final models for each response variable:

$$T_{win,j} = \alpha_{i\,[j]} + \beta_1 \,\mathrm{SD}_j + \beta_2 \,\mathrm{Slp}_i + \beta_3 \,\mathrm{BareSoil}_i + \beta_4 \,\mathrm{site}_i + \varepsilon_{ij}, \quad (1)$$

$$T_{sum,j} = \alpha_{i\,[j]} + \beta_1 \,\mathrm{Alt}_j + \beta_2 \,\mathrm{SDD}_j + \beta_3 \,\mathrm{MsT}_j + \beta_4 \,\mathrm{MicT}_j + \beta_5 \,\mathrm{LicCr}_i + \beta_6 \,\mathrm{BareSoil}_i + \varepsilon_{ij}, \quad (2)$$

$$\text{ThawD}_j = \alpha_{i\,[j]} + \beta_1\,\text{SoilMA}_j + \beta_2\,\text{Slp}_i + \beta_3\,\text{MsT}_j + \beta_4\,\text{site}_i + \varepsilon_{ij}, \quad (3)$$

where α represents the intercept, β the regression slopes of each variable, ε_{ij} is a random error term, and i and j refer to site and logger, respectively.

Model (1) explained 80.3% of the variance of T_{win} across all sites (conditional R^2), from which 66.6% is explained by fixed effects (marginal R^2) and 13.7% by random (site) effects (Table 4). The variance of the random effect ($\tau_{00} = 0.05$) is small, which indicates limited random variation among sites, while the residual variance ($\sigma^2 = 0.07$) shows only slightly larger unexplained variation within sites. Consequently, the intra-class correlation[56] was moderate (ICC = 0.41), reflecting moderate clustering among paired observations within sites. These results show that the microscale (landform-scale) heterogeneity in T_{win} is well explained while some of the inter-site (hillslope-scale) variability remains unexplained by the environmental variables. Model (1) shows that spatial variations in snow depth exert the strongest influence on GST, with a thicker snowpack leading to higher soil temperatures in winter (Figure 4a and Table 4). Increasing topographic slope also resulted in higher soil temperatures (Figure 4b and Table 4). Increasing bare soil exposure led to small, but still significant soil cooling in winter (Figure 4c and Table 4).

Model (2) explained 46.4% of the variance of T_{sum} (conditional R^2), from which 41.7% was explained by fixed effects (marginal R^2) and 4.7% by random (site) effects (Table 5). The inter-site (hillslope scale) variability in T_{sum} was well explained by the environmental variables ($\tau_{00} = 0.01$). Also, comparatively large microscale (landform-scale) heterogeneity was explained ($\sigma^2 = 0.14$, ICC = 0.08). Partial residual plots in Figure 5 show that microtopography was the dominant predictor, with a negative effect on T_{sum} (Figure 5c and Table 4) so that exposed locations ($\text{MicT}_j = 0$: hummock tops and polygon rims) tended to be warmer than sheltered locations ($\text{MicT}_j = 1$: hummock bottoms and polygon centers). As expected, increasing altitude favored lower T_{sum} (Figure 5f and Table 4). Moss thickness had a negative influence on T_{sum}, so that a thicker moss cover favored soil cooling in summer (Figure 5a and Table 4). An inverse relationship is also observed between SDD and T_{sum}, so that longer lasting snowpacks led to lower summer GST (Figure 5b and Table 4). While increasing lichen–cryptogamic crust cover led to soil cooling in summer (Figure 5e and Table 4), increasing bare soil exposure led to increasing T_{sum} (Figure 5d).

Model (3) explained 50.5% of the variance of thaw depth (conditional R^2), from which 6.5% was explained by fixed effects (marginal R^2) and 4% by random (site) effects (Table 4). The inter-site (hillslope-scale) variability in thaw depth was adequately explained by the environmental variables ($\tau_{00} = 0.05$, ICC = 0.08) but significant microscale (within-landform) heterogeneity remained unexplained ($\sigma^2 = 0.64$). Moss thickness was the dominant variable influencing thaw depth, with increasing moss thickness causing shallower thaw depths (Figure 6c and Table 4). Greater surface moisture in August and increasing topographic slope resulted in deeper thaw depths (Figure 6a,b and Table 4).

TABLE 4 Parameter estimates and statistical significance for the fitted multilevel models of winter (T_{win}) and summer (T_{sum}) ground surface temperature and thaw depth (ThawD).

	T_{win}			T_{sum}			ThawD		
Predictors	**Est**	**CI**	***p***	**Est**	**CI**	***p***	**Est**	**CI**	***p***
Intercept	1.93	1.85–2.02	<0.001	0.96	0.86–1.06	<0.001	6.12	5.68–6.56	<0.001
SD	0.9	0.73–1.08	<0.001						
SDD				−0.28	−0.47 to −0.09	0.004			
Bare soil	−0.18	−0.35 to −0.01	0.037	0.24	0.03–0.45	0.025			
Altitude				−0.34	−0.56 to −0.13	0.002			
Slope	0.19	0.0–0.38	0.047				0.79	0.35–1.22	<0.001
Microtopography				−0.41	−0.63 to −0.18	0.001			
Soil moisture							0.44	0.03–0.84	0.05
Lichen–cryptogamic crust				−0.24	−0.45 to −0.02	0.033			
Moss thickness				−0.31	−0.5 to −0.11	0.003	−0.96	−8.5 to −3.6	<0.001
Random effects									
σ^2/τ_{00}		0.07/0.05			0.14/0.01			0.64/0.05	
ICC		0.41			0.08			0.08	
N (sites)/observations		63/81			63/81			63/81	
Marginal R^2/conditional R^2		0.666/0.803			0.417/0.464			0.465/0.505	

Note: Only the potential predictors from Table 1 that were found to be statistically significant in at least one model are reported in this table. σ^2 is the residual variance, τ_{00} is the variance of the random effect, ICC is the intra-class correlation, and *N* represents the number of sites.

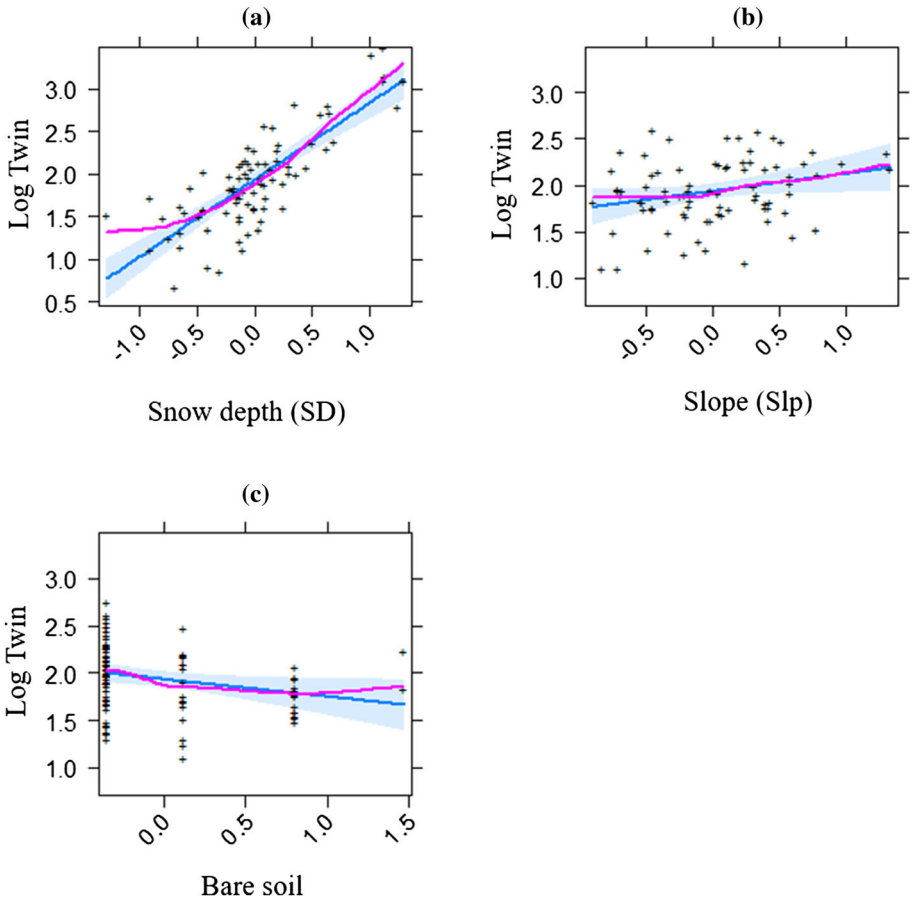

FIGURE 4 Partial residual plots for the main effects of the winter ground temperature (T_{win}) multilevel model. The *x*-axis represents the environmental variables (standardized scale) and the *y*-axis the log-transformed response variable (T_{win}). Shaded areas delineate the 95% confidence bands. (a) Snow depth (SD), (b) slope angle, and (c) bare soil. The blue line shows the expected residuals if the relationship between the predictor and response variable was linear. The pink line shows the actual residuals. [Colour figure can be viewed at wileyonlinelibrary.com]

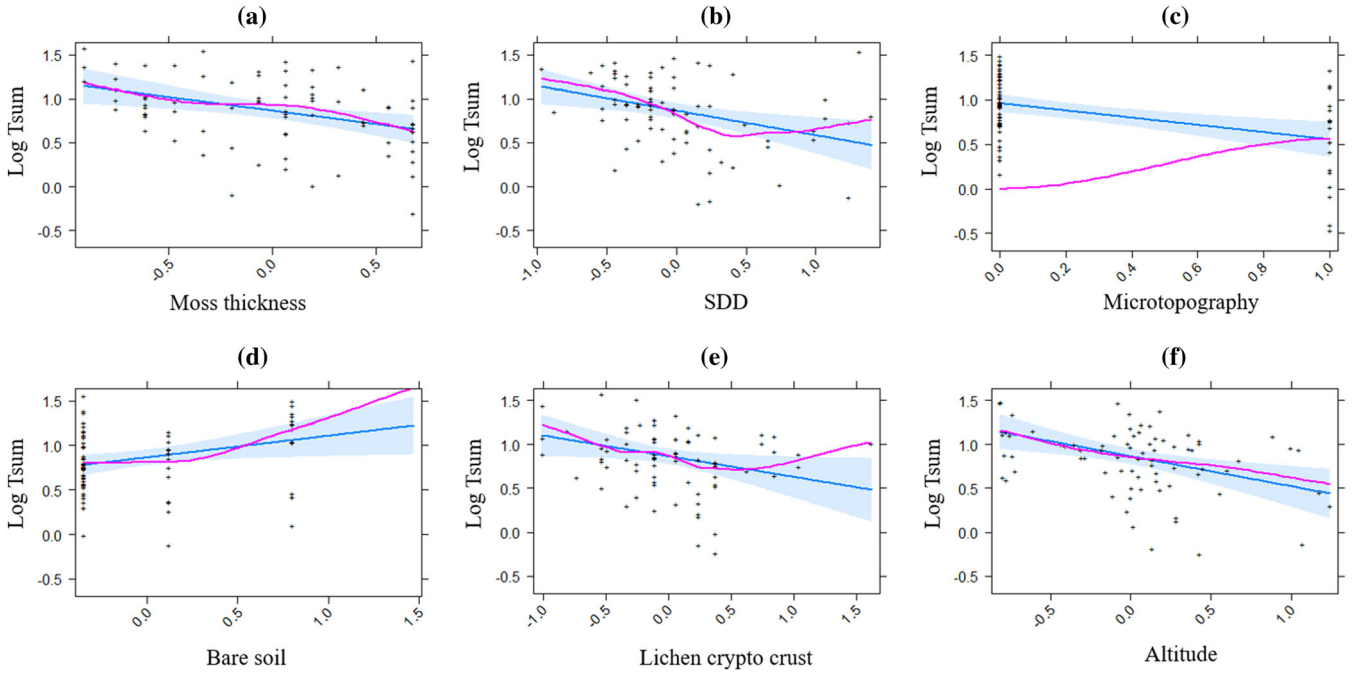

FIGURE 5 Partial residual plots for the main effects of the summer ground temperature (T_{sum}) mixed model. The *x*-axis represents the environmental variables (standardized scale) and the *y*-axis the log-transformed response variable (T_{sum}). Shaded areas delineate the 95% confidence bands. (a) Moss thickness, (b) SDD, (c) microtopography, (d) bare soil, (e) lichen–cryptogamic crust, and (f) altitude. The blue line shows the expected residuals if the relationship between the predictor and response variable was linear. The pink line shows the actual residuals. [Colour figure can be viewed at wileyonlinelibrary.com]

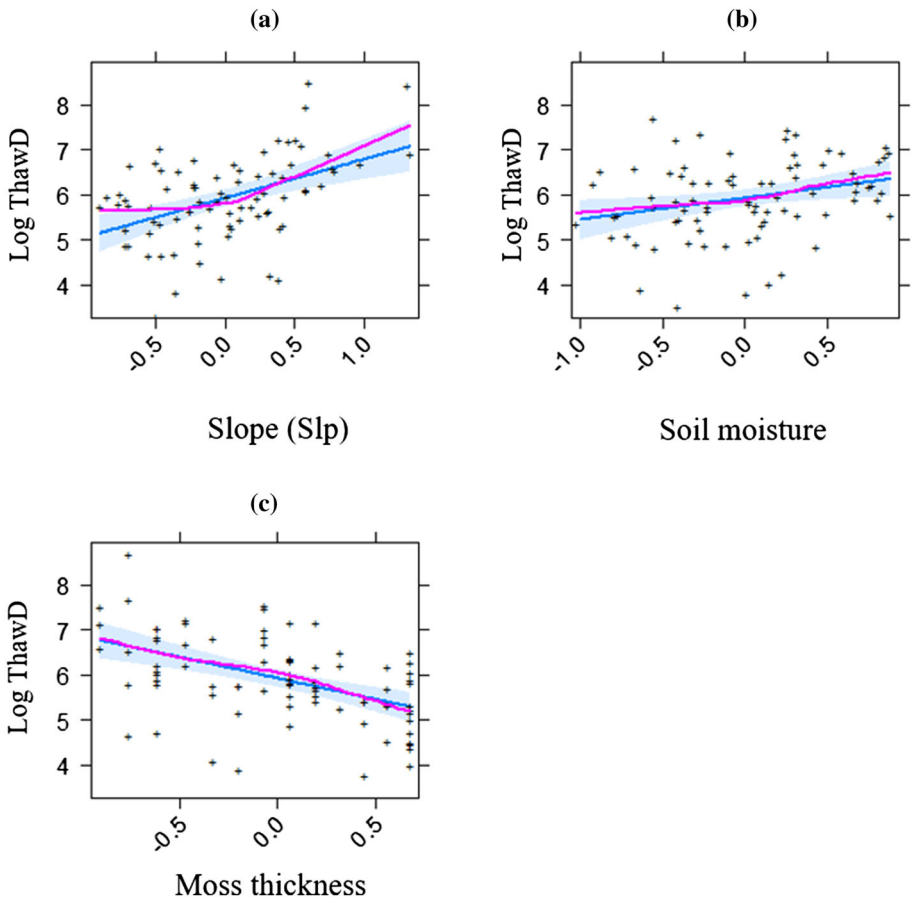

FIGURE 6 The partial residual plot of the main effects for the thaw depth mixed model. The *x*-axis represents the environmental variables and the *y*-axis the response variable (thaw depth). Colored areas indicate the confidence band (0.95). (a) Moss thickness, (b) soil moisture, and (c) slope angle. The blue line shows the expected residuals if the relationship between the predictor and response variable was linear. The pink line shows the actual residuals. [Colour figure can be viewed at wileyonlinelibrary.com]

4 | DISCUSSION

4.1 | Scale-dependent variability of GST and thaw depth

Our results showed that GST and thaw depth can vary over short distances in response to surface morphology and associated biophysical conditions. This is similar to previous findings in alpine environments such as in the eastern Swiss Alps, where mean annual GST differences of up to 2.5°C were reported over distances less than 14 m in homogeneous terrain.[30] We found greater differences over even shorter distances, that is, less than 1 m, across hummocks and polygons. Despite the significant heterogeneity of GST within these landforms, differences in mean annual GST were still larger at the hillslope scale, that is, up to 9.2°C over the elevation range of 320 m, which is also more than previously reported elsewhere for tundra environments, such as in Trail Valley Creek in the northwestern Canadian Arctic (up to 4°C within a 0.5-km^2 area),[57] in the Low Arctic Torngat Mountains of Labrador (up to 5°C over an elevation range of 420 m),[58] at Ny-Ålesund in Svalbard (up to 5.1°C over an elevation range of 500 m),[25] and over a coastal HA landscape at Cape Bounty, Nunavut (up to 8°C over an elevation range of ~150 m).[59] The hillslope-scale heterogeneity found in this study is also greater than that reported in mid-latitude mountains, such as the Swiss Alps (up to 6°C within an elevational range of 300 m)[30] and the Chilean Andes (up to 5°C).[28] This difference can be due to high snow drifting in the windswept and treeless tundra environment of Bylot Island.[25] The large spatial heterogeneity in GST and thaw depth at the micro- and hillslope scales across our study site implies that it must be carefully considered in field sampling designs as well as in remote sensing and modeling studies of tundra land surfaces.

4.2 | Environmental controls on GST and thaw depth

Spatial variations in winter GST were most pronounced at the hillslope scale than at the micro (landform) scale, with differences up to 11.6°C among landforms and up to 3.7°C within landforms. This is due to the large heterogeneity in snow depth at the hillslope scale resulting from blowing snow over the exposed tundra landscape, whereas microtopographic depressions become quickly filled by snow. This difference (11.6°C) is greater than those previously reported, for example 7.2°C at Imnavait Creek in Alaska[60] and 6.3°C at Samoylov in the Lena River Delta, Siberia,[61] due to spatial heterogeneity in snow cover. A direct preconditioning effect of the snow cover disappearance date on summer GST was also found from both the hillslope (RDA) and multiscale analyses, that is, a longer lasting snow cover led to lower GST (Figures 3 and 5 and Table 4). This finding is important and corroborates recent modeling studies that showed GSTs to be

sensitive to shifts in snow timing.[62,63] A similar phenomenon was found by Lafrenière and Lamoureux[64] on Melville Island in the Canadian HA. There, a significant inverse correlation was reported between ALT and snow depth, which was ascribed to the contrasting effects of snow cover on ALT, where the warming effect in winter (insulation) can be offset by delayed ground thawing in spring due to a thick and long-lasting snowpack.[65]

While snow cover conditions dominated the spatial variability of winter GST and also impacted summer GST, vegetation conditions were the primary driver of the spatial variability of thaw depth and also an important contributor to the spatial variability of summer GST. Despite its prostrate stature, the tundra vegetation cover had a buffering effect on GST, that is, reducing heat loss in early winter and reducing heat gains in summer over vegetated soils.[66] Moss cover and its thickness had the strongest effect on thaw depth, consistent with the known insulating effect of dry mosses.[67–69] While the summer cooling effect of mosses was apparent in the hillslope-scale RDA, it was less important than total vegetation cover (composed mostly of mosses and to a lesser extent vascular plants) (Figure 3). However, when considering also the microscale variability in the multilevel analysis, moss thickness was the most important predictor of thaw depth and one of the main drivers of summer GST spatial variability (Table 4 and Figures 5 and 6). This highlights the strong spatial heterogeneity of vegetation at the landform scale and its impact on the GST and moisture regime. For example, on mesic slopes, the sheltered and shaded hummock troughs had lower ground temperature and shallower thaw depths (Table 2). The topographic depressions between hummock tops also promote moisture accumulation, which results in ice-rich soils and favorable conditions for moss growth, which further insulates the soil; both processes lead to shallower active layers in hummock troughs (Figure S1). The vascular plant cover did not emerge as an important predictor of GST, unlike a previous study conducted in the boreal forest.[70] This is due to the low biomass and lower leaf area index of vegetation in the Arctic environment that reduce canopy shading.[59] An increased cover of lichen–cryptogamic crusts also led to little soil cooling in summer, similar to previously published results that simulated a cooling effect from lichens in the pan-Arctic region.[31]

Previous studies in Alaska and the Northwest Territories of Canada found that soil moisture modulates the cooling effect of mosses on soils.[71,72] In our case, soil moisture did not emerge as a significant predictor of summer GST both at the site-level (Figure 3) and multilevel (Figure 4) scales. Even though soil moisture did not emerge as a significant predictor of summer GST, it had a significant positive effect on thaw depth (Table 4 and Figure 6). This is similar to previous findings in the tundra of Trail Valley Creek, where soil moisture was found to promote permafrost thawing.[57] Studies conducted further south in the boreal forest also reported soil moisture to have a strong controlling influence on the soil thermal regime.[70,72] However, unlike the boreal forest where soil moisture was controlled by the balance between evapotranspiration and precipitation, soil moisture at our tundra site, as at the Trail Valley Creek site,[57] appeared to be largely controlled by snow thickness, slope position and microtopography, and not by evapotranspiration losses from vegetation, due to the low biomass (Figure S1). Contradictory effects of soil moisture appeared at the microscale: thaw depths were shallower in the moist hummock troughs and deeper on the drier tops, while the reverse occurred in the more open polygon landforms, that is, the wet centers had thaw depths deeper than the drier rims (Figure S5 and Table 2). This difference can be ascribed to topographic shading and the abundant moss cover within the encased hummock troughs, whose cooling effect dominated the increased soil heat conductivity due to soil moisture, and to more ice-rich soils, which slowed thawing in summer. The contradictory effect of soil moisture on thaw depth is consistent with a previous study in Alaska and Canada which found that while increased soil moisture increases soil thermal conductivity, which leads to deeper active layers, it also increases the latent heat of fusion for thawing.[73]

When considering the microscale variability in the multilevel models, bare ground cover emerged as a significant, albeit weak, positive predictor of GST: in winter, increased exposure of bare soil led to slight cooling, while the reverse occurred in summer, that is, warming over bare soils (Table 4 and Figures 4 and 5). This finding is similar to those reported from the McMurdo Dry Valleys of Antarctica,[74] where GSTs were higher than air temperature in summer due to solar heating of the bare ground surface, while GSTs were lower than the air in winter.

The primary topoclimatic variables controlling the surface energy balance in summer, namely altitude and solar radiation, had a small influence overall on GST. Only in summer did altitude appear as a significant predictor of GST, competing with moss thickness in importance, while solar radiation had no detectable influence. However, while hillslope-scale solar radiation was not significant, microtopographic exposure was the prime driver of summer GST variability, which in parts reflects microtopographic shading, as discussed above for hummocks. The effect of solar radiation has been shown to be modified by microtopography and the presence of mosses due to their shading and insulation effect on the ground. For example, a study conducted in the Quartermain Mountains of Antarctica[74] suggested that solar heating largely determines summer GSTs in the bare landscape, unlike the Arctic and boreal forest, where vegetation, surface organic layer, snow cover, and/or moist active layers significantly influence the relationships between atmospheric and ground thermal conditions through the surface and thermal offsets.[29,72,75]

5 | CONCLUSIONS

This research has provided a multivariable assessment of environmental effects on GST and thaw depth in a typical HA tundra environment at Bylot Island, Nunavut, Canada. Our results revealed that seasonal GST and thaw depth are highly heterogeneous, varying over short distances due to microtopography related to hummocks and ice-wedge polygons. The microscale (within-landform) variability in GST and thaw depth was large and sometimes surpassed the variability at the hillslope scale. Late-winter snowpack thickness was found to be the

prime control of winter soil temperatures due to the highly heterogeneous snow cover caused by blowing snow in this open tundra landscape. This thermal effect was found to carry over in summer through the cooling effect from a delayed snowpack disappearance. The hillslope-scale variability in snow depth was greater than at the microscale, due to landforms rapidly filling with snow. In summer a variety of environment controls, dominated by microtopographic exposure, altitude, and moss thickness determined the spatial variability of summer GST and thaw depth patterns. The microscale biophysical diversity exerted a larger influence on the spatial heterogeneity of summer GST and active layer depth, compared to winter GST.

Our results highlight the importance of considering surface feedback effects in future projections of active layer thermal conditions within heterogeneous tundra landscapes. Our results also underline the importance of accurately simulating the snow cover in future climate projections in order to properly capture the impact of snow depth and snow cover duration on permafrost temperature and thawing. Given the formidable spatial heterogeneity of the snow cover in Arctic tundra landscapes, this is still a challenging task for large-scale models. On the other hand, future increases in vegetation productivity could counteract warming-induced active layer deepening in summer, but this simple extrapolation hides the significant microtopographic heterogeneity of HA tundra environments and associated plant communities: the affinity of mosses for shaded and wet depressions exerts a dominant influence on soil temperature and thaw depths in summer. The evolution of moss cover under future climates remains a key component of active layer development in HA tundra landscapes.

ACKNOWLEDGEMENTS

This research was funded by the Natural Sciences and Engineering Research Council of Canada, Grants RGPIN-2015-03844 (C. Kinnard) and RGPIN-2015-05319 (E. Lévesque); the Canada Research Chair program, Grant 231380 (C. Kinnard); and the Centre de Recherche sur les Interactions Bassins Versants—Écosystèmes Aquatiques (RIVE) (H. Mohammadzadeh Khani). Logistical support was provided by the Polar Continental Shelf Program (Natural Resources Canada). Support from the Community of Pond Inlet, Parks Canada, and the Centre d'Études Nordiques (CEN) is acknowledged. We thank Prof. Gilles Gauthier for his logistical management of the research camp and Maria Peter, Matthieu Loyer, Denis Sarrazin, and Audrey Roy for their participation in fieldwork.

CONFLICT OF INTEREST STATEMENT

The authors have no conflicts of interest to declare.

DATA AVAILABILITY STATEMENT

The data that support the findings of this study are openly available in Centre d'Études Nordiques (CEN) at http://www.cen.ulaval.ca, reference number 10.5885/45039SL-EE76C1BDAADC4890.

ORCID

Hadi Mohammadzadeh Khani https://orcid.org/0000-0002-2707-7361

REFERENCES

1. Smith SL, Romanovsky VE, Lewkowicz AG, et al. Thermal state of permafrost in North America: a contribution to the international polar year. *Permafr Periglac Process*. 2010;21(2):117-135. doi:10.1002/ppp.690
2. Lara MJ, Nitze I, Grosse G, Martin P, McGuire AD. Reduced arctic tundra productivity linked with landform and climate change interactions. *Nat Sci Reports*. 2018;8(1):2345. doi:10.1038/s41598-018-20692-8
3. Mohammadzadeh Khani H, Kinnard C, Lévesque E. Historical trends and projections of snow cover over the High Arctic: a review. *Water*. 2022;14(4):587. doi:10.3390/W14040587
4. Williams PJ, Smith MW. *The Frozen Rarth-Fundamentals of Geocryology*. Cambridge University Press; 1989. doi:10.1017/CBO9780511564437
5. Nelson FE, Anisimov OA, Shiklomanov NI. Climate change and hazard zonation in the circum-arctic permafrost regions. *Nat Hazards*. 2002;26(3):203-225. doi:10.1023/A:1015612918401
6. International Permafrost Association. Report from the International Permafrost Association: state of permafrost in the first decade of the 21st century. *Permafr Periglac Process*. 2008;136(January):107-136. doi:10.1002/ppp
7. Smith S. Trends in permafrost conditions and ecology in northern Canada. In: *Canadian Biodiversity: Ecosystem Status and Trends 2010, Technical Thematic Report No. 9*. Canadian Councils of Resource Ministers; 2011.
8. Biskaborn B, Smith S, Noetzli J, et al. Permafrost is warming at a global scale. *Nat Commun*. 2019;2019(10):264. doi:10.1038/s41467-018-08240-4
9. Slater AG, Lawrence DM. Diagnosing present and future permafrost from climate models. *J Climate*. 2013;26(15):5608-5623. doi:10.1175/JCLI-D-12-00341.1
10. Smith SL, Burgess MM, Riseborough D, Nixon FM. Recent trends from Canadian permafrost thermal monitoring network sites. *Permafr Periglac Process*. 2005;16(1):19-30. doi:10.1002/ppp.511
11. Vonk JE, Tank SE, Bowden WB, et al. Reviews and syntheses: effects of permafrost thaw on Arctic aquatic ecosystems. *Biogeosciences*. 2015;12(23):7129-7167. doi:10.5194/bg-12-7129-2015
12. Jing-Yi Z. Snow cover influences the thermal regime of active layer in Urumqi River Source, Tianshan Mountains, China. *J Mt Sci*. 2018;15(12):2622-2636. doi:10.1007/s11629-018-4856-y
13. Chapin FS, Sturm M, Serreze MC, et al. Role of land-surface changes in Arctic summer warming. *Science*. 2005;310(5748):657-660. doi:10.1126/science.1117368
14. Aalto J, Scherrer D, Lenoir J, Guisan A, Luoto M. Biogeophysical controls on soil-atmosphere thermal differences: implications on warming Arctic ecosystems. *Environ Res Lett*. 2018;13(7):074003. doi:10.1088/1748-9326/aac83e
15. Smith SL, O'Neill HB, Isaksen K, Noetzli J, Romanovsky VE. The changing thermal state of permafrost. *Nat Rev Earth Environ*. 2022;3(1):10-23. doi:10.1038/s43017-021-00240-1
16. Belshe EF, Schuur EAG, Bolker BM, Bracho R. Incorporating spatial heterogeneity created by permafrost thaw into a landscape carbon estimate. *J Geophys Res Biogeo*. 2012;117(1):1-14. doi:10.1029/2011JG001836
17. Yi Y, Kimball JS, Chen RH, Moghaddam M, Reichle RH, Mishra U. Characterizing permafrost active layer dynamics and sensitivity to landscape spatial heterogeneity in Alaska. *Cryosphere*. 2018;12(1):145-161. doi:10.5194/tc-12-145-2018
18. Woo M. *Permafrost Hydrology*. Springer; 2012. doi:10.1007/978-3-642-23462-0
19. Sturm M, Douglas T, Racine C, Liston GE. Changing snow and shrub conditions affect albedo with global implications. *J Geophys Res*. 2005;110(G1):1-13. doi:10.1029/2005jg000013

20. Barrere M, Domine F, Decharme B, Morin S, Vionnet V, Lafaysse M. Evaluating the performance of coupled snow-soil models in SURFEXv8 to simulate the permafrost thermal regime at a high Arctic site. *Geosci Model Dev*. 2017;10(9):3461-3479. doi:10.5194/gmd-10-3461-2017
21. Van Huissteden J. *Thawing Permafrost: Permafrost Carbon in a Warming Arctic*. 1st ed. Springer Nature Switzerland AG; 2020. doi:10.1007/978-3-030-31379-1_6
22. Goodrich LE. The influence of snow cover on the ground thermal regime. *Can Geotech J*. 1982;19(4):421-432. doi:10.1029/2004RG000157
23. Zhang T. Influence of seasonal snow cover on the ground thermal regime: an overview. *Rev Geophys*. 2005;43(4):1-23. doi:10.1029/2004RG000157
24. Riseborough D, Shiklomanov N, Etzelmüller B, Gruber S, Marchenko S. Recent advances in permafrost modelling. *Permafr Periglac Process*. 2008;19(2):137-156. doi:10.1002/ppp.615
25. Gisnås K, Westermann S, Schuler TV, et al. A statistical approach to represent small-scale variability of permafrost temperatures due to snow cover. *Cryosphere*. 2014;8(6):2063-2074. doi:10.5194/tc-8-2063-2014
26. Sturm M, Holmgren J. Effects of microtopography on texture, temperature and heat flow in Arctic and sub-Arctic snow. *Ann Glaciol*. 1994;19:63-68. doi:10.1017/s0260305500010995
27. Zhang T, Frauenfeld OW, Serreze MC, et al. Spatial and temporal variability in active layer thickness over the Russian Arctic drainage basin. *J Geophys Res D Atmos*. 2005;110(16):1-14. doi:10.1029/2004JD005642
28. Apaloo J, Brenning A, Bodin X. Interactions between seasonal snow cover, ground surface temperature and topography (Andes of Santiago, Chile, 33.5°S). *Permafr Periglac Process*. 2012;23(4):277-291. doi:10.1002/ppp.1753
29. Smith MW, Riseborough DW. Climate and the limits of permafrost: a zonal analysis. *Permafr Periglac Process*. 2002;15(June 2001):1-15. doi:10.1002/ppp.410
30. Gubler S, Fiddes J, Keller M, Gruber S. Scale-dependent measurement and analysis of ground surface temperature variability in alpine terrain. *Cryosphere*. 2011;5(2):431-443. doi:10.5194/tc-5-431-2011
31. Porada P, Ekici A, Beer C. Effects of bryophyte and lichen cover on permafrost soil temperature at large scale. *Cryosphere*. 2016;10(5):2291-2315. doi:10.5194/tc-10-2291-2016
32. Elmendorf SC, Henry GHR, Hollister RD, et al. Global assessment of experimental climate warming on tundra vegetation: heterogeneity over space and time. *Ecol Lett*. 2012;15(2):164-175. doi:10.1111/j.1461-0248.2011.01716.x
33. Maxwell JB. *The Climate of the Canadian Arctic Islands and Adjacent Waters*. Environment Canada, Atmospheric Environment Service; 1982.
34. Duclos I, Lévesque E, Gratton D, Bordeleau P-A. *Vegetation Mapping of Bylot Island and Sirmilik National Park*. Vol. 136. Parks Canada; 2006.
35. Perreault N, Lévesque E, Fortier D, Lamarque LJ. Thermo-erosion gullies boost the transition from wet to mesic tundra vegetation. *Biogeosciences*. 2016;13(4):1237-1253. doi:10.5194/bg-13-1237-2016
36. Pouliot R, Rochefort L, Gauthier G. Moss carpets constrain the fertilizing effects of herbivores on graminoid plants in arctic polygon fens. *Botany*. 2009;87(12):1209-1222. doi:10.1139/B09-069
37. Ellis CJ, Rochefort L, Gauthier G, Pienitz R. Paleoecological evidence for transitions between contrasting landforms in a polygon-patterned High Arctic wetland. *Arct Antarct Alp Res*. 2008;40(4):624-637. doi:10.1657/1523-0430(07-059)[ELLIS]2.0.CO;2
38. Zoltai SC, McCormick KJ. *A Natural Resource Survey of Bylot Island and Adjacent Baffin Island, Northwest Territories*. Parks Canada; 1983.
39. CEN. Climate station data from Bylot Island in Nunavut, Canada. 2021. http://www.cen.ulaval.ca/nordicanad/dpage.aspx?doi=45039SL-EE76C1BDAADC4890
40. Fortier D, Allard M. Frost-cracking conditions, Bylot Island, eastern Canadian Arctic archipelago. *Permafr Periglac Process*. 2005;16(2):145-161. doi:10.1002/ppp.504
41. Gagnon CA, Cadieux M-C, Gauthier G, Lévesque E, Reed A, Berteaux D. *Analyses and Reporting on 15 Years of Biological Monitoring from Bylot Island*. Vol. 47. Sirmilik National Park of Canada; 2010.
42. Braun-Blanquet J. In: Fuller GD, Conard HS, eds. *Plant Sociology: The Study of Plant Communities*. 1st ed. Bibliolife DBA of Bibilio Bazaar II LLC; 1932.
43. Burt R. *Soil Survey Field and Laboratory Methods Manual*. U.S. Department of Agriculture, Natural Resources Conservation Service; 2009. https://www.nrcs.usda.gov/wps/PA_NRCSConsumption/download?cid=stelprdb1244466&ext=pdf
44. Rowell DL. *Soil Science: Methods and Applications*. Wiley; 1994.
45. Shean DE, Alexandrov O, Moratto ZM, et al. An automated, open-source pipeline for mass production of digital elevation models (DEMs) from very-high-resolution commercial stereo satellite imagery. *ISPRS J Photogramm Remote Sens*. 2016;116:101-117. doi:10.1016/j.isprsjprs.2016.03.012
46. Marti R, Gascoin S, Berthier E, De Pinel M, Houet T, Laffly D. Mapping snow depth in open alpine terrain from stereo satellite imagery. *Cryosphere*. 2016;10(4):1361-1380. doi:10.5194/tc-10-1361-2016
47. Staub B, Delaloye R. Using near-surface ground temperature data to derive snow insulation and melt indices for mountain permafrost applications. *Permafr Periglac Process*. 2016;28(1):237-248. doi:10.1002/ppp.1890
48. Legendre P, Birks HJB, Lotter AF, Juggins S, Springer S. From classical to canonical ordination. In: Birks H, Lotter A, Juggins S, Smol J, eds. *Tracking Environmental Change Using Lake Sediments*. Developments in Paleoenvironmental Research. Vol. 5. Springer; 2012. doi:10.1007/978-94-007-2745-8_8
49. Ter Braak CJF. Canonical community ordination. Part I: basic theory and linear methods. *Ecosci*. 1994;1(2):127-140. doi:10.1080/11956860.1994.11682237
50. Legendre P, Oksanen J, ter Braak CJF. Testing the significance of canonical axes in redundancy analysis. *Methods Ecol Evol*. 2011;2(3):269-277. doi:10.1111/j.2041-210X.2010.00078.x
51. Gelman A, Hill J. In: Alvarez RM, Beck NL, Wu LL, eds. *Data Analysis Using Regression and Multilevel/Hierarchical Models*. Cambridge University Press; 2018.
52. Zuur AF, Ieno EN, Walker NJ, Saveliev AA, Smith GM. *Mixed Effects Models and Extensions in Ecology with R*. Vol. 173. Springer; 2010. doi:10.1111/j.1467-985x.2010.00663_9.x
53. Pinheiro JC, Bates DM. *Mixed-Effects Models in S and S-Plus*. Springer Science & Business Media; 2000. doi:10.1007/978-1-4419-0318-1
54. Crawley MJ. *The R Book*. 2nd ed. Wiley; 2010. doi:10.1016/b978-0-12-374507-1.00050-9
55. Cohen J. *Statistical Power Analysis for the Behavioral Sciences*. Academic Press; 1977.
56. Nakagawa S, Johnson PCD, Schielzeth H. The coefficient of determination R^2 and intra-class correlation coefficient from generalized linear mixed-effects models revisited and expanded. *J R Soc Interface*. 2017;14(134):1-11. doi:10.1098/rsif.2017.0213
57. Grünberg I, Wilcox EJ, Zwieback S, Marsh P, Boike J. Linking tundra vegetation, snow, soil temperature, and permafrost. *Biogeosciences*. 2020;17(16):4261-4279. doi:10.5194/bg-17-4261-2020
58. Davis E, Trant A, Hermanutz L, et al. Plant–environment interactions in the low Arctic Torngat Mountains of Labrador. *Ecosystems*. 2021;24(5):1038-1058. doi:10.1007/s10021-020-00577-6
59. Garibaldi MC, Bonnaventure PP, Lamoureux SF. Utilizing the TTOP model to understand spatial permafrost temperature variability in a

High Arctic landscape, Cape Bounty, Nunavut, Canada. *Permafr Periglac Process*. 2021;32(1):19-34. doi:10.1002/ppp.2086
60. Sturm M, Holmgren J. Effects of microtopography on texture, temperature and heat flow in Arctic and sub-Arctic snow. *Int Glaciol Soc Eff*. 1994;19:63-68. doi:10.3189/1994AoG19-1-63-68
61. Gouttevin I, Langer M, Löwe H, Boike J, Proksch M, Schneebeli M. Observation and modelling of snow at a polygonal tundra permafrost site: spatial variability and thermal implications. *Cryosphere*. 2018; 12(11):3693-3717. doi:10.5194/tc-12-3693-2018
62. Jan A, Painter SL. Permafrost thermal conditions are sensitive to shifts in snow timing. *Environ Res Lett*. 2020;15(8):1-12. doi:10.1088/1748-9326/ab8ec4
63. Rixen C, Høye TT, Macek P, et al. Winters are changing: snow effects on Arctic and alpine tundra ecosystems. *Arct Sci*. 2022;8(3):572-608. doi:10.1139/as-2020-0058
64. Lafrenière MJ, Laurin E, Lamoureux SF. The impact of snow accumulation on the active layer thermal regime in high arctic soils. *Vadose Zone J*. 2013;12(1):vzj2012.0058. doi:10.2136/vzj2012.0058
65. Park H, Fedorov AN, Zheleznyak MN, Konstantinov PY, Walsh JE. Effect of snow cover on pan-Arctic permafrost thermal regimes. *Climate Dynam*. 2015;44(9-10):2873-2895. doi:10.1007/s00382-014-2356-5
66. Heijmans MM, Magnússon RI, Lara MJ, et al. Tundra vegetation change and impacts on permafrost. *Nat Rev Earth Environ*. 2022;3(1): 68-84. doi:10.1038/s43017-021-00233-0
67. Voortman BR, Bartholomeus RP, van Bodegom PM, Gooren H, van der Zee SEATM, Witte JPM. Unsaturated hydraulic properties of xerophilous mosses: towards implementation of moss covered soils in hydrological models. *Hydrol Process*. 2014;28(26):6251-6264. doi:10.1002/hyp.10111
68. Turetsky MR, Bond-Lamberty B, Euskirchen E, Talbot J, Frolking S, Mcguire AD. The resilience and functional role of moss in boreal and arctic ecosystems. *New Phytol*. 2012;196(1):49-67. doi:10.1111/j.1469-8137.2012.04254.x
69. Hrbáček F, Cannone N, Kňažková M, Malfasi F, Convey P, Guglielmin M. Effect of climate and moss vegetation on ground surface temperature and the active layer among different biogeographical regions in Antarctica. *Catena*. 2020;190(February):104562. doi:10.1016/j.catena.2020.104562
70. Williams M, Zhang Y, Estop-Aragonés C, et al. Boreal permafrost thaw amplified by fire disturbance and precipitation increases. *Environ Res Lett*. 2020;15(11):114050. doi:10.1088/1748-9326/abbeb8
71. O'Donnell JA, Romanovsky VE, Harden JW. The effect of moisture content on the thermal conductivity of moss and organic soil horizons from black spruce ecosystems in interior Alaska. *Soil Sci*. 2009; 174(12):646-651. doi:10.1097/SS.0b013e3181c4a7f8
72. Fisher JP, Estop-Aragones C, Thierry A, et al. The influence of vegetation and soil characteristics on active-layer thickness of permafrost soils in boreal forest. *Glob Chang Biol*. 2016;22(9):3127-3140. doi:10.1111/gcb.13248
73. Clayton LK, Schaefer K, Battaglia MJ, et al. Active layer thickness as a function of soil water content. *Environ Res Lett*. 2021;16(5):055028. doi:10.1088/1748-9326/abfa4c
74. Lacelle D, Lapalme C, Davila AF, et al. Solar radiation and air and ground temperature relations in the cold and hyper-arid Quartermain Mountains, McMurdo Dry Valleys of Antarctica. *Permafr Periglac Process*. 2016;27(2):163-176. doi:10.1002/ppp.1859
75. Way RG, Lewkowicz AG. Environmental controls on ground temperature and permafrost in Labrador, northeast Canada. *Permafr Periglac Process*. 2017;29(2):73-85. doi:10.1002/ppp.1972

SUPPORTING INFORMATION

Additional supporting information can be found online in the Supporting Information section at the end of this article.

How to cite this article: Khani HM, Kinnard C, Gascoin S, Lévesque E. Fine-scale environment control on ground surface temperature and thaw depth in a High Arctic tundra landscape. *Permafrost and Periglac Process*. 2023;1-14. doi:10.1002/ppp.2203